JOURNAL OF PROPULSION AND POWER
Vol. 19, No. 5, September–October 2003

Dynamic and Nonlinear Simulation of Liquid-Propellant Engines

H. Karimi*
Khaje Nassir-Al-Deen Toosi University of Technology, 16579 Tehran, Iran
A. Nassirharand†
Farab Company, 15946 Tehran, Iran
and
M. Beheshti‡
University of Tehran, 14174 Tehran, Iran

A new dynamic and nonlinear simulation method for liquid-propellant engines is presented, and the corresponding software for a particular engine is developed. The logic of the simulation method and the software is based on following the liquid(s). The dynamic equations of motion are composed of implicit nonlinear algebraic equations, as well as nonlinear and time-varying differential equations. The implicit nonlinear algebraic equations are solved using a number of nested Newton–Raphson loops, and the nonlinear and time-varying differential equations are solved using a first-order Euler technique. The simulation results are compared with experimental results. The software language is FORTRAN, and it is composed of approximately 200 subroutines for a total of approximately 4000 lines.

Nomenclature

$A_{1,t}$	=	combustion chamber throttle area, m^2
A_5	=	defined intermediate variable for the fuel pump head equation [see Eq. (3)]
$a_{1,1}$, $a_{1,2}$	=	product of an orifice discharge coefficient and the orifice area, m^2
a_5	=	one of the coefficients of the fuel pump head equation
B_5, C_5	=	defined intermediate variable for the fuel pump head equation [see Eqs. (6) and (8)]
b_5, c_5	=	coefficients of the fuel pump head equation
$b_{5,2}$	=	exit width of fuel pump impeller, m
C_1^*	=	characteristic speed, m/s
C_2	=	$\sqrt{(2W_{2,\mathrm{sp}})}$, J/Kg
D_4	=	turbine diameter, m
$\mathrm{d}m_1$	=	accumulated mass in the combustion chamber, kg
g	=	gravity constant, 9.81m/s^2
H_5	=	fuel pump head, m
$H_{5,p}$	=	nominal fuel pump head, m
J_{eq}	=	turbopump equivalent moment of inertia, Kg · m^2
K_{EL}	=	see Eq. (26)
$K_{5,z}$	=	effect coefficient of the fuel pump blade
k_1, k_2	=	adiabatic constant, combusion chamber and gas generator
L_1^*	=	characteristic length, m
m_1	=	mass in the combustion chamber [see Eq. (17)], kg
$\dot{m}$	=	dummy mass flow rate, kg/s
$\dot{m}_{1,e}$, $\dot{m}_{1,i}$	=	combustion chamber exit and inlet mass flow rate, kg/s
$\dot{m}_{1,\mathrm{fu}}$	=	exit fuel mass flow rate of combustion chamber injectors, kg/s
$\dot{m}_{1,\mathrm{ox}}$	=	exit oxidizer mass flow rate of combustion chamber injectors, kg/s
$\dot{m}_2$	=	gas generator exit mass flow rate, kg/s
O/F	=	ratio of the oxidizer mass flow rate to that of the fuel
P_1	=	pressure inside the combustion chamber, Pa
$P_{1,\mathrm{binj,fu}}$	=	pressure just before the fuel injectors of the combustion, chamber Pa
$P_{1,\mathrm{binj,ox}}$	=	pressure just before the oxidizer injectors of the combustion chamber, Pa
P_2	=	pressure inside the gas generator, Pa
$P_{4,\mathrm{st}}$	=	turbine exit static pressure while the gas generator is working, Pa
Q_5	=	volumetric flow rate of the fuel pump, m^3/s
$Q_{5,p}$	=	nominal volumetric flow rate of the fuel pump [see Eq. (4)], m^3/s
$q_{5,p}$	=	defined intermediate parameter in terms of nominal values of the fuel pump
R_1, R_2	=	gas constant of combusion products of the combustion chamber and of the gas generator, J/(kg · K)
T_1, T_2	=	temperature of the combustion chamber and gas generator chamber, K
TQ_2	=	external torque due to the gas generator acting on the turbopump N · m
TQ_3	=	external torque due to the starter acting on the turbopump [see Eq. (10) and change subscript 2 to 3], N · m
TQ_5	=	fuel pump torque acting on the turbopump, N · m
TQ_6	=	oxidizer pump torque acting on the turbopump [see Eq. (13) and change subscript 5 to 6], N · m
t	=	time, s
u	=	$(D_4/2)\omega$, m/s
$V(t)$	=	instantaneous volume of liquid in an element [see Eq. (17)], m^3
V_1	=	volume of the combustion chamber, m^3
$\bar{V}$	=	see Eq. (27)
$W_{2,\mathrm{sp}}$	=	adiabatic work due to gas generator, J/Kg
$\beta_{5,2\pi}$	=	exit angle of the fuel pump blade, rad
Γ_1	=	function of k_1 [see Eq. (21)]
γ_5	=	$\rho_{\mathrm{fu}} \cdot g$, kg/$m^2 \cdot s^2$
ΔP	=	dummy pressure difference, Pa
η_2	=	gas generator efficiency
η_5	=	efficiency of the fuel pump
$\eta_{5,zp}$	=	hydraulic efficiency of the fuel pump
ρ, ρ_{fu}, ρ_{ox}	=	liquid, fuel, and oxidizer densities, kg/m^3
τ	=	dummy delay time, s

Received 5 July 2002; revision received 3 March 2003; accepted for publication 8 April 2003.

*Assistant Professor, Mechanical Engineering Department; control727@yahoo.com.
†Technical Expert, Mechanical and Civil Department.
‡Graduate Student, Mechanical Engineering Department.

τ_1 = combustion delay time, s
ω = turbopump angular speed, rad/s
ω_p = nominal angular speed of the turbopump, rad/s

Introduction

LIQUID-PROPELLANT engines (LPEs) form an important part of aerospace systems. These types of engines are utilized when high performance and high specific impulse are required. The number of published works in the open literature indicate that simulation of LPEs is not a new field in rocket engineering. An overview of typical LPE modeling and simulation publications follow. In the literature, detailed model of LPE combustion chamber and models for prediction of combustion chamber instabilities,[1–6] modeling mixing and combustion processes at near-critical conditions,[7] prediction of mass flow rate and heat addition in a LPE during initial portion of a LPE start phase,[8] analysis of turbulent incompressible flow in a pipe for use in an LPE,[9] analysis of coaxial injector flow,[10] development of cavitation models,[11] development of static models for all components of the engine,[12] analysis of fatigue failure,[13] analysis of LPE turbomachinery,[14,15] and analysis of engine feed system,[16–18] are considered.

In the mentioned literature, modeling is done in such a way that application of a numerical integration technique is adequate to solve the equations of motion. For example, in Ref. 7, a unified framework for modeling purposes in terms of a governing system of integro–differential equations is developed, and the governing equations are solved via a special method of discretizing. Similarly, other related simulation literature,[16–18] unlike the work presented herein, also rely on pure discretization of the model; this requires modeling to be done in terms of a set of integro–differantial equations. Execution costs of the corresponding simulation codes would be difficult to justify when a complicated model is not required.

In general, the simulation task begins after a mathematical model of the system is developed. Also the required mathematical model is tied to the particular application of interest. For some applications, a detailed model is required, and in some other applications, a simplified model would suffice. For example, as a rule of thumb, to design a robust control system, a dynamic and nonlinear model that would approximate the response of the variable to be controlled within approximately 20% of its actual value would suffice.[19,20] A simplified model of an LPE, as demonstrated in the "Mathematical Model" section, is composed of coupled and implicit algebraic and differential equations.

To the best of our knowledge, this is the first paper that presents a simulation algorithm for liquid-propellant engines that are modeled in terms of implicit and coupled nonlinear algebraic and differential equations. In summary, the simulation algorithm is based on forming a set of first-order nested Newton–Raphson loops inside an Euler intergration routine; the logic for formation of the nested Newton–Raphson loops is systematic, and it is based on following the liquid in its path. Normally, such set of equations of motion is solved by application of a nonlinear algebraic equation solver (which is usually based on a quasi-Newton approach) inside a numerical integration routine.[21] Our research efforts in usage of such an approach using either a customized or commericially available software (such as MATLAB®) were not successful, and we experienced convergence problems. Also, usage of commericially available simulation environments (such as SIMULINK), on inexpensive platforms (1500-MHz computers), required unreasonable execution times for tasks such as design of a reliable, robust, and microprocessor-based combustion chamber pressure control system. Hence, the need for an alternative solution technique was detected. Note that there are no restrictions that would limit the application of the developed algorithm to other types of models; however, verification of this hypothesis is left for future work.

The problem statement follows: Given the coupled and implicit nonlinear algebraic and differential dynamic equations of motion of a liquid-propellant engine, what is an efficient numerical method for solving these equations and developing the associated software? The primary contributions of this research are twofold: 1) the algorithm for solving the coupled and implicit equations of motion and 2) the developed software that simulates a particular liquid-propellant engine. Comparison between simulation results and those of experiments are presented.

Operation of Liquid-Propellant Engines

Before we continue, the operation of liquid-propellant engines is described. Consider the schematic diagram of a typical existing open-cycle liquid-propellant engine that is rich in fuel (low O/F) as shown in Fig. 1. This particular engine uses an aviation hydrocarbon fuel C_nH_m with a high boiling point. The maximum thrust

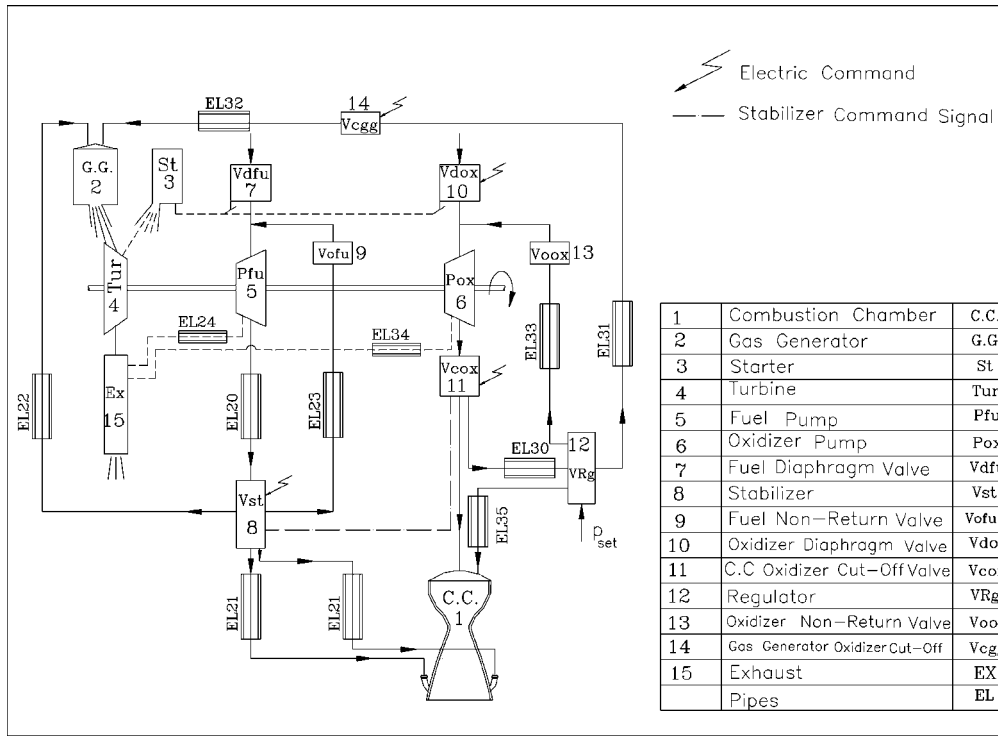

1	Combustion Chamber	C.C.
2	Gas Generator	G.G.
3	Starter	St
4	Turbine	Tur
5	Fuel Pump	Pfu
6	Oxidizer Pump	Pox
7	Fuel Diaphragm Valve	Vdfu
8	Stabilizer	Vst
9	Fuel Non–Return Valve	Vofu
10	Oxidizer Diaphragm Valve	Vdox
11	C.C Oxidizer Cut–Off Valve	Vcox
12	Regulator	VRg
13	Oxidizer Non–Return Valve	Voox
14	Gas Generator Oxidizer Cut–Off	Vcgg
15	Exhaust	EX
	Pipes	EL

Fig. 1 Schematic diagram of liquid-propellant engine.

of such engines is approximately 400 kN, and the maximum combustion chamber pressure is about 75×10^5 Pa. Such engine cycles are demonstrated in Ref. 22.

The engine elements are divided into four subgroups. Those are 1) valve, 2) turbopump, 3) combustion chamber and gas generator, and 4) piping system. (In the following description, the numbers are referenced to Fig. 1). The operation of the engine starts by an electric command that starts a combustion in the starter 3. This combustion generates pressurized gas that opens the diaphragm valves 7 and 10, and it also turns the turbine 4. Consequently, the shaft of the turbopump starts rotating, and the pumps 5 and 6 start pumping fuel and oxidizer into the system. Now, consider the two fuel and oxidizer paths. In the fuel path, fuel enters the stabilizer control valve 8, and the output of this valve is a controlled amount of fuel toward the combustion chamber and the gas generator. At the same time, in the oxidizer path, oxidizer passes through the cutoff valve 11, and it enters the combustion chamber. The fuel and oxidizer that have entered the combustion chamber produce the required thrust via combustion. This thrust must be controlled. The amount of oxidizer that enters the gas generator 2 controls the thrust, and the desired amount of oxidizer that must flow through the gas generator is utilized via the regulator control valve. This oxidizer, along with the fuel that has entered the gas generator from the fuel path, produce combustion; this combustion results in a pressurized gas that keeps the turbine running when the starter leaves the circuit. The angular speed of the turbine controls the amount of fuel and oxidizer flow toward the combustion chamber.

Note that, once the operation of a particular liquid-propellant engine is mastered, the operations of other types of liquid-propellant engines become self-explanatory by looking at the corresponding schematic diagrams; various types of liquid-propellant engines function similarly.

Mathematical Model

The primary purpose of this section of the paper is to give an overall perspective of the complexity of equations of motion. A complete development of equations of motion is beyond the scope of the paper. There are approximately 210 equations in 210 unknowns. The primary assumptions behind the developed model follow.

1) Turbulance in combustion is not considered.

2) Heat transfer to the walls in the combustion chamber and the gas generator is neglected. Let the stay time of gas in chambers be very short.

3) Interaction between gas and liquid is neglected.

4) The gas flow in the combustion chamber and gas generator is assumed to be adiabatic and inviscid.

5) The gas pressure drops in the combustion chamber and the gas generator due to viscous friction at the walls, as well as the inertia of the gas column, are neglected. Let the length of the liquid path in the combustion chamber and the gas generator be short, and let the magnitude of the gas velocity be small.

6) The time required for fluid change to gas in the combustion chamber and the gas generator is assumed to be in the range of 0.001–0.01 s.

7) The fluids have high boiling points, and therefore, all fluid paths are of a liquid type. Hence, there is no need for a model of gas pipes and orifices.

8) The fuel and oxidizer injector fillings are negligible, that is, centrifugal single-base injectors are used.

9) Compressibility of the fluid is not taken into account.

10) Effects of cavitaion in pumps are neglected.

11) Temparature effects are neglected.

12) Vortex flow in the incompressible fluid is not considered.

13) All elements are assumed to be rigid.

14) The bandwidth of the model is about 50 Hz. See Ref. 23 for process pseudo frequency response.

15) Pipe dynamics are neglected.

16) The mass flow rate is considered uniform in each circuit branch at a given time step.

17) Turbulent flows are assumed in pipes. At steady-state conditions, the flows in pipes would be turbulent, and during transient conditions the flows may momentarily become laminar with effects that are assumed to be negligible.[18]

18) The exit pressure rise of an element being filled with liquid is neglected until that elelment is filled.

19) The energy equation is indirectly taken into account as discussed in the "Combustion Chamber and Gas Generator" subsection.

20) Without loss of generality, the dynamics of the internal movable hydromechanical parts are neglected.

21) Density and viscocity of the fluid are assumed to be constants.

As mentioned, the elements of a liquid-fueled engine are divided into four subgroups. For each subgroup, the mathematical model of a particular candidate element is briefly described.

Valve Subgroup

The candidate element from this group is the regulator control valve. The purpose of this valve is to control the pressure inside the combustion chamber. This is a fairly complex valve, and its nonlinear mathematical model is composed of a series of equations resulting from the application of conservation of mass and momentum, as well as the Newton laws of motion. For demonstration of the simulation algorithm, a simple orifice model is used to describe in- and outflow modulation.

Turbopump

The exit pressurized gas of the gas generator rotates the turbine, and the turbine commissions the pumps. The rotation of the shaft causes the fluid to be pumped and exits the pumps at a higher pressure. The fuel pump head H_5 is calculated from

$$H_5 = \left(a_5 + b_5 Q_5 - c_5 Q_5^2\right)/g \tag{1}$$

where

$$a_5 = A_5 \omega^2 \tag{2}$$

$$A_5 = (0.97 + 0.8 q_{5,p})\left(H_{5,p}/\omega_p^2\right) \tag{3}$$

$$q_{5,p} = 1 \Big/ \left(1 + \frac{2\pi H_{5,p} b_{5,2} \tan(\beta_{5,2\pi})}{Q_{5,P} \omega_p K_{5,z} \eta_{5,zp}}\right) \tag{4}$$

$$b_5 = B_5 \omega \tag{5}$$

$$B_5 = (0.325 - 0.8 q_{5,p})\left(H_{5,p}/\omega_p^2\right)(Q_{5,p}/\omega_p)^{-1} \tag{6}$$

$$c_5 = C_5 \tag{7}$$

$$C_5 = 0.296\left(H_{5,p}/\omega_p^2\right)/(Q_{5,p}/\omega_p)^2 \tag{8}$$

The equations of motion for the turbine consists of application of D'Lambert's law as well as equations for determination of external torques acting on the turbopump. These equations are[18]

$$J_{\text{eq}} \dot{\omega} = TQ_2 + TQ_3 - TQ_5 - TQ_6 \tag{9}$$

$$TQ_2 = (1/\omega) \cdot \dot{m}_2 \cdot W_{2,\text{sp}} \cdot \eta_2 \tag{10}$$

$$W_{2,\text{sp}} = k_2/k_2 - 1 \cdot R_2 \cdot T_2 \cdot \left[1 - (P_{4,\text{st}}/P_2)^{(k_2-1)/k_2}\right] \tag{11}$$

$$\eta_2 = 0.004 + 2.676(u/C_2) - 2.928(u/C_2)^2 \tag{12}$$

$$TQ_5 = \gamma_5 H_5 Q_5 / \omega \eta_5 \tag{13}$$

Combustion Chamber and Gas Generator

To obtain the equations of motion of the combustion chamber, first the mass balance equation is written as

$$\dot{m}_{1,i}(t - \tau_1)\,\mathrm{d}t = \dot{m}_{1,e}(t)\,\mathrm{d}t + \mathrm{d}m_1 \tag{14}$$

When it is noted that $\dot{m}_{1,i}(t-\tau_1) = \dot{m}_{1,\text{fu}}(t-\tau_1) + \dot{m}_{1,\text{ox}}(t-\tau_1)$, and the preceding equation is divided by $\mathrm{d}t$, the following equation

is obtained:

$$\dot{m}_{1,i}(t-\tau_1) = \dot{m}_{1,\mathrm{fu}}(t-\tau_1) + \dot{m}_{1,\mathrm{ox}}(t-\tau_1) = \dot{m}_{1,e}(t) + \frac{\mathrm{d}m_1}{\mathrm{d}t} \tag{15}$$

The characteristic speed C_1^* is defined as

$$C_1^* = P_1 A_{1,t}/\dot{m}_{1,e} \tag{16}$$

The perfect gas law is

$$m_1 = P_1 V_1/R_1 T_1 \tag{17}$$

Now assume that $R_1 T_1$ is constant: The following equation is obtained by taking the derivative of Eq. (17) with respect to time:

$$\frac{\mathrm{d}m_1}{\mathrm{d}t} = \frac{V_1}{R_1 T_1} \cdot \frac{\mathrm{d}P_1}{\mathrm{d}t} \tag{18}$$

The characteristic length is defined as

$$L_1^* = V_1/A_{1,t} \tag{19}$$

The characteristic speed may be written as

$$C_1^* = \sqrt{R_1 T_1}/\Gamma_1 \tag{20}$$

where, in the relation (20),

$$\Gamma_1 = \sqrt{k_1}[2/(k_1+1)]^{(k_1+1)/2(k_1-1)} \tag{21}$$

When Eqs. (19) and (20) are substituted into Eq. (18), the following equation is obtained:

$$\frac{\mathrm{d}m_1}{\mathrm{d}t} = \frac{L_1^* A_{1,t}}{C_1^{*2}\Gamma_1^2} \cdot \frac{\mathrm{d}P_1}{\mathrm{d}t} \tag{22}$$

When Eqs. (16) and (22) are substituted Eq. (15), the following equation is obtained:

$$\frac{L_1^* A_{1,t}}{\Gamma_1^2 C_1^{*2}} \cdot \frac{\mathrm{d}P_1}{\mathrm{d}t} + \frac{A_{1,t}}{C_1^*} P_1 = \dot{m}_{1,\mathrm{fu}}(t-\tau_1) + \dot{m}_{1,\mathrm{ox}}(t-\tau_1) \tag{23}$$

Equation (23) is the equation of motion of the combustion process. For a given P_1 and O/F, the values of T_1, C_1^*, k_1, and R_1 are computed offline and are incorporated as tables of values into the computer model. In other words, the energy equation is taken into account via the earlier mentioned off-line computations that result from the combustion of the used fuel and oxidizer. Then, as simulation time marches ahead, the needed mentioned values for a given P_1 and O/F are obtained by linear interpolation. To use the same combustion model for the gas generator, experimental results should be used to employ correction factors to adjust the mentioned computed offline values. Note that because precise pipe dynamics are not employed, the delay time in Eq. (23) may be set equal to zero.

There are also two hydraulic equations that relate to the element under study:

$$\dot{m}_{1,\mathrm{ox}} = a_{1,1}[2\rho_{\mathrm{ox}}(P_{1,\mathrm{binj,ox}} - P_1)]^{0.5} \tag{24}$$

$$\dot{m}_{1,\mathrm{fu}} = a_{1,2}[2\rho_{\mathrm{fu}}(P_{1,\mathrm{binj,fu}} - P_1)]^{0.5} \tag{25}$$

Piping System

The pipes are modeled by the following familiar equation:

$$\dot{m} = K_{EL}\sqrt{2\rho\Delta P} \tag{26}$$

Simulation Algorithm

In a typical engine, the liquid tank pressure (pressure at the inlet of the diaphragm valves) and the downstream pressure, for example, the combustion chamber pressure and/or the gas generator pressure, are known; therefore, one is able to solve the hydraulic circuit, and the values of pressures and flow rates of the circuit may be determined. The developed simulation algorithm follows.

1) Define the first Newton–Raphson loop. The start of the loop is at the exit of the diaphragm valve; if the liquid path till the first node is not filled, the end of the loop is at the exit of the element that is being filled. In this case, solve the hydraulic circuit and go to step 6. Otherwise, the end of the loop is at the end of the following node. In this step, the existing pressure value at the exit of the diaphragm valve must be used. (Initial value would be 1 atm.) If there are no dividing nodes in the liquid path to the combustion chamber and/or the gas generator, with the existing pressure value at the exit of the diaphragm valve, solve the circuit and compute the combustion chamber and/or the gas generator pressure; then go to step 5. Note that, in this case, there would only be one Newton–Raphson loop, and the end of the loop is inside the combustion chamber and/or the gas generator, whichever is applicable.

2) With the known input tank pressure and the existing inlet pump pressure of step 1, solve the hydraulic circuit until a dividing node of the liquid occurs. With reference to Fig. 1, with the known input tank pressure and the assumed pump inlet pressure, the circuit is solved until the exit of the cutoff valve 11.

3) For each path of the dividing node, define a new Newton–Raphson loop nested with the previous one. (Note that if another dividing node is reached while following the initial divided path, the user needs to define another nested Newton–Raphson loop and so on.)

4) Solve the hydraulic circuit of the dividing paths. (At this point the pressures and mass flow rates of the dividing circuits would be known.)

5) For the case where there are no dividing nodes, correct the pump inlet pressure value of step 1 until the computed combustion chamber and/or the gas generator that is computed from step 1 equals the actual combustion chamber and/or the gas generator pressure. (Note that the actual pressure value of the preceding step is used, and this value is computed by integration of the combustion chamber equations.) If there are dividing points, check the conservation of mass at the end of the first Newton–Raphson loop. If the conservation of mass is satisfied, go to step 6; otherwise, correct the value of the pump inlet pressure using the Newton–Raphson algorithm and go to step 1.

6) If the final simulation time is reached, then stop; otherwise, integrate the equations of motion, and go to step 1.

Description of the Main Program

The flow chart of the main program is shown in Fig. 2. In the first step, all required input coefficients are read in from an ASCII file. These values are written into an output file so the user could check the correctness of the input values. Then, the initial values of all variables (including state variables) are set. For example, all pressures are set equal to 1 atm. Next, the time loop starts. At the beginning of this loop, the values of the selected variables are written into an output file; this file is postprocessed in the MATLAB environment. Then, the variable limits are imposed. The next step is the key step of the main program, and it consists of integrating the equations of motion. The integration technique is the simple Euler method. After integration, the table of variables, whose delayed values are required, are generated. This table keeps the values of the selected variables as a function of time. At the times that simulation code is at time t and the code needs the value at time $t-\tau$, the simulation code gets the required delayed values from this table. Then, the simulation time marches ahead, and the position of the sensing diaphragm of the stabilizer control valve is computed. The last step of the main loop is that if the simulation time has not reached its final time, the main loop is repeated; otherwise, the execution of the code terminates.

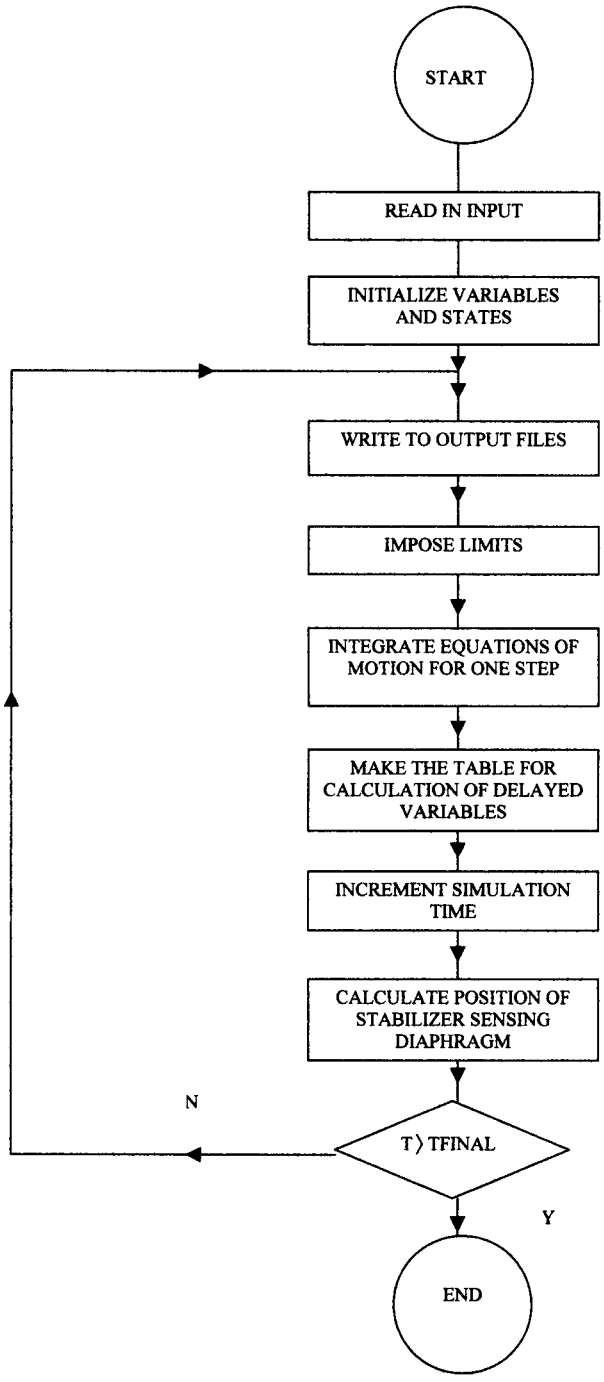

Fig. 2 Flow chart of the main program.

Demonstration Example Problem

To demonstrate the application of the developed simulation algorithm, consider the schematic diagram of the engine shown in Fig. 1. In the beginning, before the starter exit gas opens the diaphragm valve 10, the pump entrance pressure equals 1 atm. After the diaphragm valve is opened, liquid begins to fill valve 10. As long as this valve is being filled, the liquid does not reach the pump, and again the pump entrance pressure equals 1 atm. To see if an element is filled with liquid, the following equation is used:

$$\frac{d\bar{V}}{dt} = \frac{1}{\rho V}\dot{m}, \qquad 0 \le \left[\bar{V} = \frac{V(t)}{V}\right] \le 1 \tag{27}$$

Note that Eq. (27) needs to be integrated as long as $\bar{V} < 1$; otherwise, this equation is not integrated.

Once valve 10 is filled, according to step 1 of the algorithm, the first Newton–Raphson loop is defined. The start of the loop is at the exit of the diaphragm valve, and the end of the loop is at the exit of the pump. Use the known pressure value at the inlet of the diaphragm valve and the pressure value at the exit of the pump (which equals 1 atm) to solve the circuit in the following fashion.

1) Guess the inlet pressure of the pump. The first guess would equal 1 atm. For subsequent guesses, use the most recent available value.

2) With the known pressure at the inlet of the diaphragm valve 10 and the existing pressure at the inlet of the pump, compute the fluid mass flow rate entering the pump.

3) With the known pump inlet pressure, pump inlet mass flow rate, and the speed of the pump, compute the pump outlet pressure. Note that speed of the pump is a state variable, and its value from the preceding step is used.

4) If the computed pump outlet pressure from part 3 equals 1 atm, then it may be concluded that existing pump inlet pressure value is correct, and the circuit is solved. Otherwise, correct the existing value of the pump inlet pressure according to the Newton-Raphson algorithm, and go to part 2.

Once the value of the pressure at the exit of the pump is solved for, go to step 6. Step 6 integrates the equations of motion, and directs the user back to step 1. This cycle between steps 1 and 6 continues until the cutoff valve 11 is filled. According to step 1, the start of the first Newton–Raphson loop would be as before, and the end of that loop would be at the first dividing node, that is, the exit of the cutoff valve 11.

In step 2, with the existing pressure value at inlet of the pump, the circuit is solved till the exit of the cutoff valve. In step 3, two other Newton–Raphson loops nested with the first one are defined. One loop starts at the exit of the cutoff valve and ends inside the combustion chamber. The other loop starts at the exit of the cutoff valve and ends at the exit of the element that is being filled and is in the path toward the gas generator. If the regulator valve were not modeled as an orifice, then, according to step 3, one would have to define a third Newton–Raphson loop nested with the second one due to liquid divisor node inside the regulator. In that case, the second Newton–Raphson loop would end at the liquid division point inside the regulator, and three other Newton–Raphson loops, nested with the second one, would have been defined. The third level Newton-Raphson loops would start at the liquid division point inside the regulator. Then, the end of one of these loops would have been at the exit of the element that was being filled and that was in the path of the combustion chamber, the end of one other loop would have been at the exit of the element that was being filled and that was in the path of the gas generator, and, finally, the end of the last one of these loops would have been at the exit of the element that was being filled and that was in the path toward the inlet of the pump.

According to step 4, the hydraulic circuit from the exit of the cutoff valve 11 until inside the combustion chamber is solved. (The pressure at the exit of the cutoff valve was calculated in step 2, and the combustion chamber pressure is a state variable and its earlier value is used.) Similarly, the circuit from the exit of the cutoff valve toward the gas generator is solved.

From step 4, liquid mass flow rates leaving the cutoff valve 11 are known; from step 2, the liquid mass flow rate entering the cutoff valve is also known. According to step 5, the conservation of mass at the cutoff valve 11 is checked. If the conservation of mass at the cutoff valve 11 is satisfied, then go to step 6. Otherwise, correct the pump inlet pressure value via the Newton–Raphson method and go to step 1.

In step 6, the equations of motion are integrated; if final simulation time is reached, then stop. Otherwise, go to step 1.

Comparison of the Simulation and Experimental Results

The test stand experimental results of an existing engine (of the type described earlier) are compared with the corresponding simulation results of that same engine. The accuracy of the measured data is estimated to be ±2%. The per cent errors in steady-state values are given in Table 1. The accuracy of the transient response behavior is demonstrated by Figs. 3–6. Note that discrepancies between

Table 1 Error in experiment and simulation steady-state engine variable values

Description	%Error
Turbopump speed	0.27
Pressure inside gas generator	0.62
Fuel mass flow rate of gas generator	0.56
Oxidizer mass flow rate of gas generator	2.35
Combustion chamber pressure	2.54
Fuel mass flow rate of combustion chamber	0.69
Oxidizer mass flow rate of combustion chamber	3.65
Exit pressure of fuel pump	2.77
Exit pressure of oxidizer pump	0.26
Turbine power	0.71

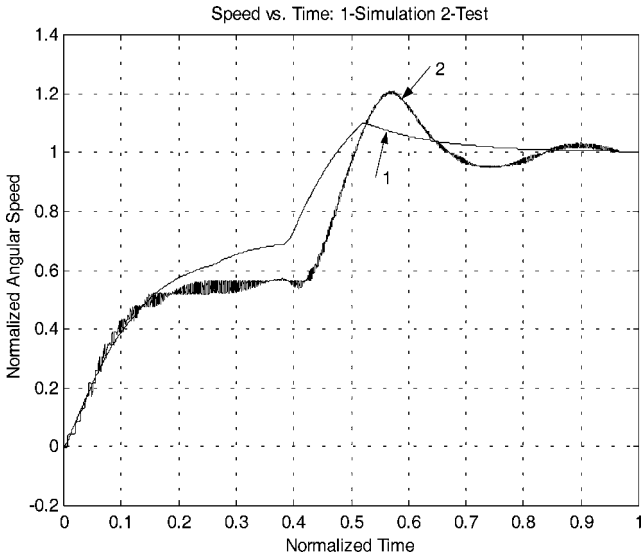

Fig. 3 Comparison of 1) simulation and 2) experimental time responses of turbopump speed.

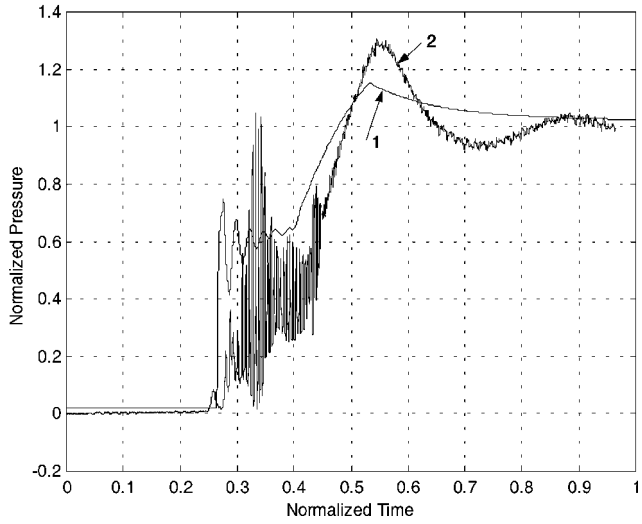

Fig. 4 Comparison of 1) simulation and 2) experimental time responses of combustion chamber pressure.

the transient behaviors are not due to the newly developed solution procedure. The hypothesis describing the origin of the mentioned discrepancies is that the regulator valve is modeled as an orifice and that corresponding compensating action of the valve is neglected. The effect of this assumption is amplified in Fig. 5, where the compensating dynamics of the regulator valve (from the time regulator becomes active until the time regulator assumes steady state conditions), which dynamically excite the gas generator, have not been taken into account. This hypothesis may be verified by analyzing

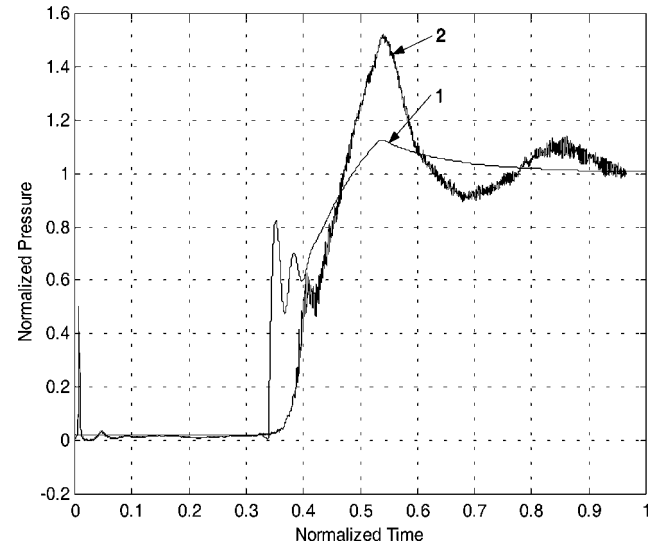

Fig. 5 Comparison of 1) simulation and 2) experimental time responses of gas generator pressure.

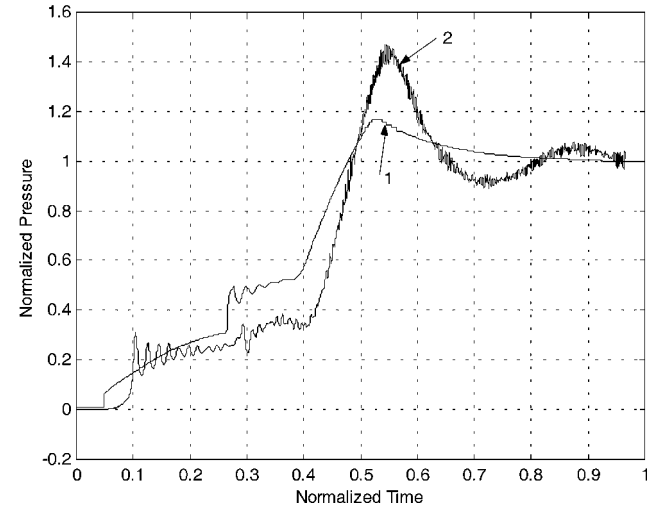

Fig. 6 Comparison of 1) simulation and 2) experimental time responses of the exit oxidizer pump pressure.

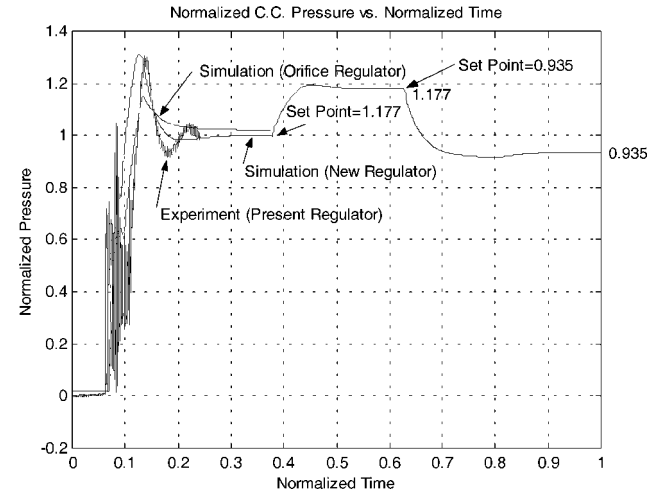

Fig. 7 Verification of discrepancy hypothesis,[20] normalized combustion chamber pressure vs normalized time.

the results reported in Ref. 20. In that work, a microprocessor-based control system is designed to replace the existing complicated hydromechanical feedback structure of the regulator valve. Figure 7 shows the simulation results by including the dynamics of the designed controller, and a closer agreement between simulation and test results is obtained. Figure 7 also shows the pressure response behavior of the combustion chamber at different pressure setpoints.

Summary

A new approach for simulation of liquid-fueled engines is developed and described in detail. The developed simulation algorithm is composed of six primary steps, and it is based on the use of nested single-variable Newton–Raphson loops inside a numerical integration routine. The application of the simulation algorithm to a specific simple engine model is demonstrated. The execution time of the software is fairly fast, about 20 s on a 1500-MHz microprocessor that facilitates such tasks as robust control system design. Such tasks do not require precise dynamic models. A list of recommendations follow.

1) Investigate the applicability of the developed simulation algorithm to more complicated models that take into account pipe dynamics, dynamics of dividing liquid points, and more complicated combustion and turbo-pump models.

2) Develop of a general purpose software package for simulation of liquid-propellantengines based on the developed simulation algorithm.

3) Develop of a general purpose software utility that would solve a set of nonlinear algebraic equations via a number of nested single-variable Newton–Raphson loops instead of globally applying a standard technique such as a quasi-Newton method. The primary advantages of such an approach would be faster execution time and an increase in the probability of convergence as described in the Introduction section.

References

[1]Osherov, A., Natan, B., and Gany, A., "Analytical Modeling of the Gas Generator Frequency Response in Hybrid Rocket Boosters," *Acta Astronautica,* Vol. 39, No. 8, 1996, pp. 589–598.

[2]Bentsman, J., and Pearlstein, A. J., *Active Noise and Vibration Control*, Vol. 8, Winter Annual Meeting, American Society of Mechanical Engineers, New York, 1990, pp. 31–42.

[3]Jiang, T. L., and Chiu, H.-H., "Bipropellant Combustion in a Liquid Rocket Combustion Chamber," *Journal of Propulsion and Power*, Vol. 8, No. 5, 1992, pp. 995–1003.

[4]Ivancic, B., and Mayer, W., "Time- and Length Scales of Combusion in Liquid Rocket Thrust Chambers," *Journal of Propulsion and Power*, Vol. 18, No. 2, 2002, pp. 247–253.

[5]Habiballah, M., Lourme, D., and Pit, F., "PHEDRE: Numerical Model for Combustion Stabiulity Studies Applied to the Ariane Viking Engine," *Journal of Propulsion and Power*, Vol. 7, No. 3, 1991, pp. 322–329.

[6]Wang, T.-S., "Unified Navier–Stokes Flowfield and Performance Analysis of Liquid Rocket Engines," *Journal of Propulsion and Power*, Vol. 9, No. 5, 1993, pp. 678–685.

[7]Oefelein, J. C., and Yang, V., "Modeling High-Pressure Mixing and Combustion Processes in Liquid Rocket Engines," *Journal of Propulsion and Power*, Vol. 14, No. 5, 1998, pp. 843–857.

[8]Avampato, T. J., and Saltiel, C., "Dynamic Modeling of Starting Capabilities of Liquid Propellant Rocket Engines," *Journal of Propulsion and Power*, Vol. 11, No. 2, 1995, pp. 292–300.

[9]Haskew, J. T., and Sharif, M. A. R., "Performance Evaluation of Vaned Pipe Bends in Turbulent Flow of Liquid Propellants," *Applied Mathematical Modelling*, Vol. 21, No. 1, 1997, pp. 48–62.

[10]Mayer, W., and Kruelle, G., "Rocket Engine Coaxial Injector Liquid/Gas Interface Flow Phenomena," *Journal of Propulsion and Power*, Vol. 11, No. 3, 1995, pp. 513–518.

[11]Maitre, T., and Kueny, J. L., "Three-Dimensional Models of Cavitation in Rocket Engine Inducers," *Fluid Machinery*, Vol. 96, Winter Annual Meeting, American Society of Mechanical Engineers, New York, 1990, pp. 49–53.

[12]Tishin, A. P., and Gurova, L. P., "Liquid Rocket Engine Modeling," *Soviet Aeronautics*, Vol. 32, No. 3, 1989, pp. 99–101.

[13]Newlin, L., Sutharshana, S., Ebbeler, D., Moore, N., Fox, E., Annis, C., and Creager, M.,"Probabilistic Low Cycle Fatigue Failure Analysis with Application to Liquid Propellant Rocket Engines," *Structures, Structural Dynamics and Materials Conference*, Pt. 2, AIAA, Washington, DC, 1990, pp. 1115–1123.

[14]McDaniel, D. M., and Snellgrove, L. M., "Liquid Propulsion Turbomachinery Model Testing," *Aerospace Engineering*, Vol. 12, No. 7, 1992, pp. 8–12.

[15]Chen, W.-C., Chan, D., Brozowski, L. A., Lee, G., Hsu, W., and Anthony, H., "CFD as a Turbomachinery Design Tool: Code Validation," *Fluids Engineering and Laser Anemometry Conference*, Vol. 227, American Society of Mechanical Engineers, New York, 1995, pp. 67–74.

[16]Lin, T. Y., and Baker, D., "Analysis and Testing of Propellant Feed System Priming Process," *Journal of Propulsion and Power*, Vol. 11, No. 3, 1995, pp. 505–512.

[17]Kun, L., and Yulin, Z., "A Study on Versatile of Liquid Propellant Rocket Engine Systems Transients," *Proceedings of 36th Joint Propultion Conference and Exhibit on Disc* [CD-ROM], AIAA, Wasington, DC, 2000.

[18]Beliayev, E. N., Chevanov, V. K., and Chervakov, V. V., *Mathematical Modeling of Working Process in Liquid Propellant Rocket Engines,* Moscow Aviation Inst. Publications, Moscow, 1999 (in Russian), pp. 38–50, 85–143.

[19]Taylor, J. H., "A Systematic Nonlinear Controller Design Method Based on Quasilinear System Models," *American Control Conference*, IEEE Publications, Piscataway, NJ, 1983, pp. 141–145.

[20]Nassirharand, A., and Karimi, H., "Design of a Single-Range Controller for the Pressure Control of a Combustion Chamber," *Scientica Iranica Journal*, (to be published).

[21]Reklaitis, G. V., Ravindran, A., and Ragsdell, K. M., *Engineering Optimization*, Wiley, New York, 1983, pp. 112–117.

[22]Sutton, G. P., *Rocket Propulsion Elements*, Wiley, New York, 1992, pp. 145–158.

[23]Nassirharand, A., and Karimi, H., "Input/Output Characterization of Highly Nonlinear Systems," *Advances in Engineering Software*, Vol. 33, Nos. 11–12, 2002, pp. 825–830.